Design of an innovative Polymerase Chain Reaction device based on buoyancy driven flow

Elena BIANCHI[1,2*], Margherita CIOFFI [1,3], Katia LAGANÀ[1], Gabriele DUBINI[1]

* Corresponding author: Tel.: ++39 02 23994283; Fax: ++39 02 23994286; Email: ebianchi@stru.polimi.it
1 Laboratory of Biological Structure Mechanics, Department of Structural Engineering, Politecnico di Milano, Italy
2 Department of Biomedical Engineering, Politecnico di Milano, Italy
3 IRCCS Istituto Ortopedico Galeazzi, Italy

Abstract Polymerase Chain Reaction (PCR) plays a central role in the field of molecular biology. The miniaturization of PCR systems is promising as it potentially minimizes costly reagent consumption and time required for analysis. In PCR microdevices a sample solution is usually handled by external pumps. An alternative solution relies on temperature-induced density difference in the presence of a body force to induce buoyancy driven flow. This alternative method is easy to be used and does not require expensive set-up, but, to date, the thermo-fluid-dynamic field in the micro-channels still needs to be optimized. The present study focuses on the design of micro-channels, having innovative and optimized shapes to obtain proper fluid actuation and DNA sample amplification within buoyancy driven flow PCR devices. A parametric study is carried out by means of computational thermal fluid dynamic modeling: several channel geometry configurations were compared in terms of time required for analysis, temperature distribution and priming volume. The advantages and disadvantages of such configurations are discussed.

Keywords: Buoyancy Driven flow, Polymerase Chain Reaction, CFD, DNA amplification

1. Introduction

Since 1983 the Polymerase Chain Reaction (PCR) has been playing a central role in the field of molecular biology. It is a powerful tool for creating large numbers of copies of specific DNA fragments for applications like DNA fingerprinting, genomic cloning and genotyping for disease diagnosis (Mullis 1990). The common devices used for PCR consist of metal blocks that are continually able to thermally cycled between three distinct temperatures for denaturation (90-94 °C), annealing (50-60 °C) and extension (72 °C). The advantage of these block thermal cyclers is that they can simultaneously amplify 96-384 samples placed in wells that are sandwiched between the thermal block and cover plate. The disadvantage associated with this format is the poor thermal management which leads to limitations on the speed of the amplification. Moreover the need for manually pipetting reagents into the wells limits the minimum volume of PCR reaction to about 0.5ml (Chen et al., 2005). In the last few years the limitations of benchtop thermal cyclers have been overcome thanks to the development of microfluidic PCR devices. These systems can generally be classified into two categories: the chamber type, where the DNA sample is placed and thermally cycled, and the continuous flow type, which consists of microchannels continuously looped through different temperature zones. The continuous flow type has the important advantage to being able to guarantee better thermal management (since each temperature required for the PCR is at equilibrium prior to target amplification); this positively affects amplification time reduction (Park et al., 2003). However continuous flow PCR devices require external pumping and have a fixed number of thermal cycles. In this light some alternative solutions have been recently developed, relying on a temperature-induced density difference in the presence of a body force to induce buoyancy driven flow (Wheeler et al, 2004; Krishnan et al, 2002; Krishnan et al, 2004). This alternative method is easy to be used and does

not require expensive set-up, but, to date, further efforts should be addressed to optimize the thermo-fluid-dynamic field in the micro-channels. The main issue to be addressed is the thermal cycling process control.
The present study focuses on the design of micro-channels, having innovative and optimized shapes to obtain proper fluid actuation and DNA sample amplification within buoyancy driven flow PCR devices.
This paper reports a parametric study carried out by means of computational thermal fluid dynamic modeling. Several channel geometry configurations were compared in terms of time required for analysis, temperature distribution and priming volume. Also advantages and disadvantages of such configurations are discussed.

2. Materials and Methods

A three dimensional microchannel was arranged in a closed loop (Fig. 1): different combinations of microchannel square cross-sections (W = 500, 400 and 200 µm), and device length (L = 3, 4 and 5 mm) were modelled. The solid modeler GAMBIT (Ansys Inc., Canonsburg, PA, USA) was used to set up the models and build the meshes. For each geometry configuration two domains were built: the fluid domain, within the microchannels, was considered to have the same properties as an aqueous solution (Table 1). The solid domain, in the centre of the device, consisted of a polymeric material, having the same properties as poly-dimethyl siloxane (PDMS in Table 1). Geometries have been discretized with about 70000 elements, resulting from sensitivity and optimization analyses. The Boussinesq approximation was applied to fluid density, with a reference temperature T_0= T1 = 330 K. Material properties are taken from the literature (Incropera et al, 2006; Gui et al, 2006).
Steady state simulations were carried out using the finite volume code FLUENT (Ansys Inc., Canonsburg, PA, USA).
In the fluid domain, the Navier-Stokes equations for incompressible Newtonian fluids were solved:

$$\begin{cases} \rho_0(\vec{v}\cdot\nabla)\vec{v} = -\nabla P + \mu\nabla^2\vec{v} + \rho_0\beta(T-T_0)\vec{g} \\ \nabla\cdot\vec{v} = 0 \end{cases} \quad (1)$$

where $\vec{v}$ and p are the velocity vector and pressure, respectively; ρ_0 is the density of the flow at the reference temperature T_0 and $\vec{g}$ is the gravity due to the acceleration.
In both fluid and solid domains heat transfer equations were solved respectively as :

$$Water \quad \rho_0 c_p(\vec{v}\cdot\nabla)T = k\nabla^2 T \quad (2)$$

$$PDMS \quad \nabla^2 T = 0 \quad (3)$$

where c_p is the specific heat coefficient at constant pressure and k is the conduction coefficient. Gravitational acceleration was considered to be 9.8 ms^{-2} parallel to L. No slip conditions were imposed at the walls. Heater positioning was simulated by imposing constant-temperature boundary conditions (T1 and T2, 367 K and 330 K respectively) on one side of the device (Fig. 1). Thermal continuity was applied at the wall between the microchannel and the PDMS core. Thermal resistances were applied at the other boundaries, so as to simulate conduction through a PDMS layer (5 mm in thickness) and the external environment (air at 297 K with a convection coefficient h = 5 $Wm^{-2}K^{-1}$).

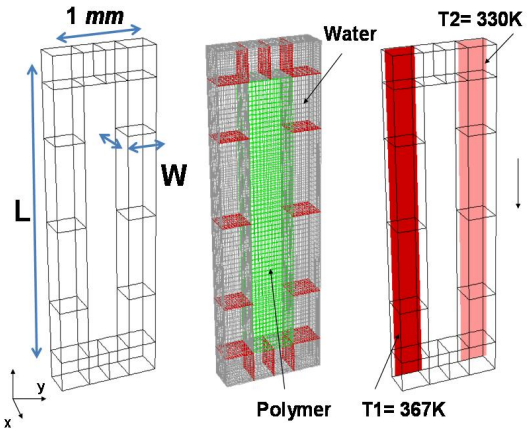

Fig. 1. Schematic of the designed microfluidic device, with mesh and thermal boundary conditions.

Table 1. Material Properties (Incropera et al, 2006; Gui et al, 2006).

Water		PDMS	
cp (J/kgK)	4180	cp (J/kgK)	1460
ρ (kg/m^3)	1050	ρ (kg/m^3)	900
K (W/mK)	0.684	K (W/mK)	0.15
μ (Pa s)	$1 \cdot 10^{-3}$		
β (1/K)	$6.16 \cdot 10^{-4}$		

3. Results

Figure 2 shows the velocity maps on the middle cross-sectional plane (normal to the X axis) of the designed microdevices .

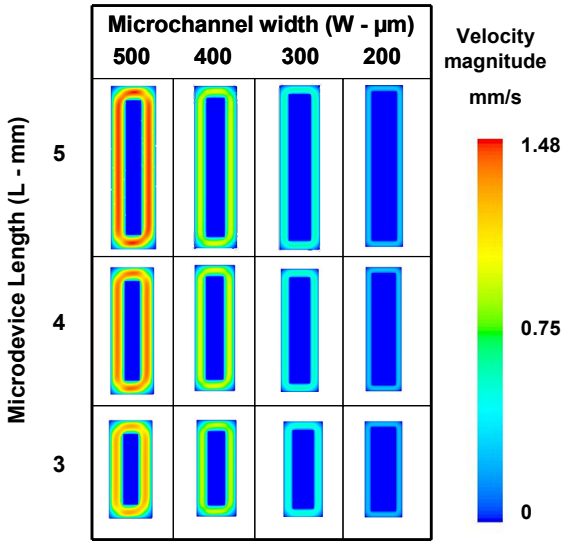

Fig. 2. Velocity contours on the middle cross-sectional plane of the designed microdevices.

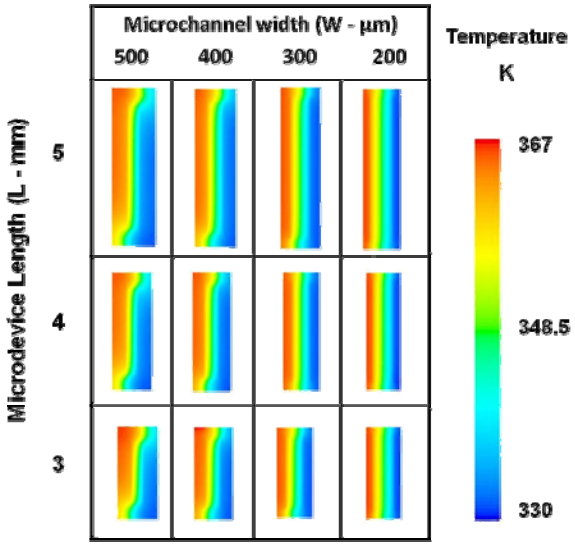

Fig. 3. Temperature contours on the middle cross-sectional plane of the designed microdevices.

The average velocity increases with increasing channel length (L) and increasing microchannel width (W): it ranges from 0.73 mm/s for a loop with W = 0.5 mm and L = 5 mm to 0.12 mm/s for a loop with W = 0.2 mm and L = 3 mm. Temperature maps on the same plane are represented in Figure 3. As expected, loops with lower average velocities (smaller W) exhibit a more symmetric temperature distribution.

Figure 4 shows a graph reporting the time required for a single thermal cycle in each condition. The microdevice, with L = 5 mm and W = 0.2 mm, requires the maximal time for a single cycle (89 seconds). Minimum cycle time is acquired by the microdevice with L = 3 mm and W = 0.5 mm.

Figure 5 reports the priming volume of each device versus microchannel cross section, for the different geometry configurations. The priming volume ranges from 0.3 to 3 μl.

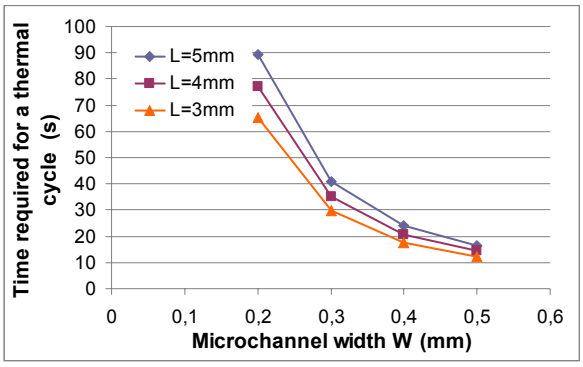

Fig. 4. Time required for each thermal cycle versus microchannel width W. Different microdevice lengths are considered.

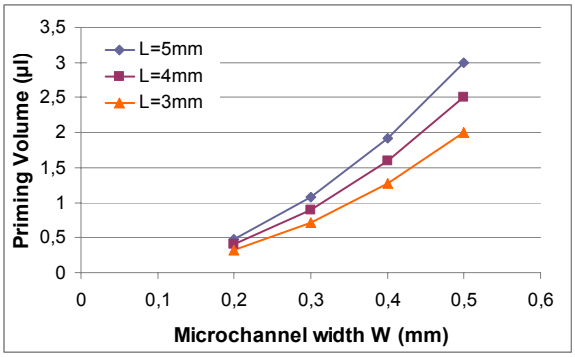

Fig. 5. Device priming volume versus microchannel width W. Different microdevice lengths are considered.

The devices with smaller W show an homogenous temperature distribution within

the microchannel cross-section, as shown in Figure 6.

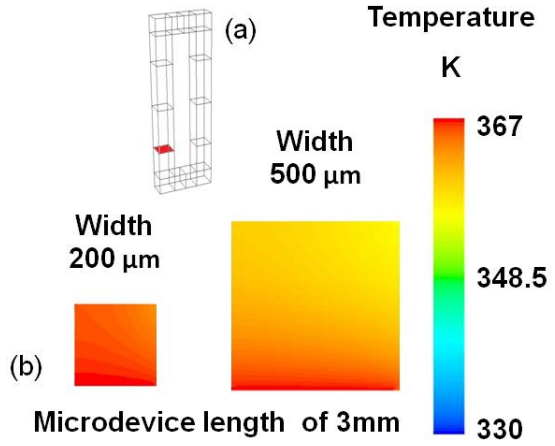

Fig.6 Temperature contours (b) on a comparative cross section (a) in microdevice models with the same L and different W .

4. Discussion

In the present work a design optimization of buoyancy driven flow PCR microdevices was carried out by means of computational thermal fluid dynamic modeling.

Recent studies showed that CFD modeling can be successfully used to optimize the geometry configuration of other types of PCR microdevices, such as continuous flow designs (Li et al, 2006; Gui et al, 2006; Wang et al, 2005). In particular, Gui et al. (2006) highlighted the potential of thermal modeling in evaluating the best material (polymer, silicon or glass) and the more appropriate device thickness to achieve a homogenous temperature within an electroosmosis-based continuous flow device. Wang and collaborators (2005) quantified the effect of the applied flow rate on temperature distribution within an external pressure driven PCR microsystem.

A few examples of buoyancy driven flow PCR microdevices have been published (Krishnan et al, 2002; Krishnan et al, 2002; Wheeler et al, 2004; Chen et al, 2004).

In particular Wheeler and collaborators experimentally demonstrated the feasibility to amplify DNA samples (90-160 base pairs) by means of a closed loop where the flow was induced by buoyancy forces. Two heaters were applied to the device, in order to obtain a cycle with two phases, 95 °C (denaturation) and 60 °C (annealing). The sample can flow through the 95 °C phase (denaturation) and 60 °C (annealing) phase for variable number of cycles. Thereafter the extension phase is achieved by soaking the sample at 72 °C for 3 min. However, in Wheeler's study the configuration geometry was not optimized in order to enhance the PCR performances, related to temperature distribution, cycle time and priming volume.

In the present study we have considered a closed loop able to cycle a DNA sample between the annealing and denaturation phases. After cycling, the flow may be stopped and the extension phase may be achieved by setting both heaters at 72 °C.

The computational modelling of the thermal cycle showed that widening the channel cross section significantly increases the flow velocity, consequently reducing the time required for a single cycle. Also increasing channel length leads to an increase of the flow velocity, but it also increases the length of the cycle. For the channel lengths considered, this results in an increase of the time required for a cycle. Previous studies (Krishnan et al, 2002; Wheeler et al, 2004) reported thermal cycles of 10-30 s. One might infer that the ideal device should minimize the time required for amplification, such as the device studied with channel length equal to 5 mm and channel width equal to 0.5 mm. This system will allow for a DNA amplification of 2 µl of DNA sample solution in approximately 12 s. However such configuration leads to a non homogenous temperature distribution within the channels, which may prevent efficient DNA amplification. Therefore we suggest to go for systems with smaller channel cross-sections, such as the microdevice with L = 3 mm and W = 0.4 mm (time for a single cycle = 18 s; priming volume = 1.3 µl). Experimental tests are under way to validate the simulated fluid-dynamics and thermal distribution and to ultimately evaluate the efficacy of such configuration.

The present work has a number of limitations which should be addressed in future. The

simulations evaluated only the steady state behaviour of the designed microdevices. Transient analyses should also be carried out for a better understanding of the device performance. Comparative simulations with varying polymeric thicknesses of the device should be also envisaged. In fact thinner systems could be preferable as they could be more easily integrated in lab on a chip devices.
Efforts should be made to further optimize the proposed geometry configuration. The potential of including the extension area (72 °C) in the microchannel loop should be investigated through further simulations. A study by Chen and collaborators (2004) simulated a buoyancy driven flow PCR where all three thermal phases were included. However, the geometrical configuration of the system was not designed in order to optimize each phase time. In fact, the time limiting factor for the reaction is the extension phase. In contrast to denaturation and hybridization, which occur almost instantly, the length of the extension phase is restricted by the 100 nucleotide per second extension rate of the Taq enzyme. Previous studies on continuous flow PCR set the time ratio of the sample to each temperature zone to 1:2:4 for denaturation, hybridization, and extension, respectively (Li et al, 2006). Depending on the length of the DNA segments to be amplified, a minimum extension time can be chosen. Thereafter, a loop having different cross sections for each thermal phase could be easily designed and computationally optimized through parametric thermal fluid dynamic simulations.

4. Conclusions

Computational fluid dynamic simulations have been carried out to study buoyancy driven flow phenomena inside a micro channel having an innovative shape and conceived to allow the optimization of DNA sample amplification within PCR devices.
Steady state simulations have been performed to identify the parameters affecting the length and the timing of the thermal cycle. As expected, both the width of the channel cross section W and the length of the channel L increased the flow velocity. However, increasing L resulted also in augmenting the total length of the cycle, ultimately increasing the cycle time. As a consequence of the higher velocity, a large cross section implies an inhomogeneous temperature distribution that results in an uncontrolled thermal condition for the sample flowing in the device. Heat transfer through the PDMS layer to the environment affects the temperature profile inside the channel in a negligible way, due to the considerable thickness of the wall.
The results of this study can help choosing a few geometry configurations, which potentially optimize the performance of a PCR microdevice, reducing the cycle time and the priming volume, with homogeneous distribution of temperature within the channel cross sections.
Future developments of this study may mainly address the optimization such types of microdevice geometry, for the case of introduction of a third thermal condition (extension at 72 °C).

References

Chen Z., Qian S., Abrams W. R., Malamud D., Bau H. H. 2004 .Thermosiphon-Based PCR Reactor: Experiment and Modeling Anal. Chem. 76, 3707-3715

Chen J., Wabuyele M., Chen H., Patterson D., Hupert M. et al. 2005. Electrokinetically synchronized polymerase chain reaction microchip fabricated in polycarbonate. Anal Chem. 77(2):658-66.

Gui L. and Ren CL. 2006. Numeric Simulation of Heat Transfer and Electrokinetic Flow in an Electroosmosis-Based Continuous Flow PCR Chip. Anal. Chem. 78, 6215-6222.

Incropera F. P., Dewitt D. 2006. Fundamentals of heat and mass transfer.

Li S., Fozdar D. Y. , Ali M. F., Li H., Shao D., Vykoukal D. M , J. Vykoukal, Floriano P. N., Olsen M., McDevitt J. T,Gascoyne P. R. C, Chen S., 2006 A Continuous-Flow Polymerase Chain Reaction Microchip With Regional Velocity Control, journal of microelectromechanical systems, vol. 15, no. 1, February 223

Krishnan M., Ugaz Victor, A Mark, Burns, 2002. PCR in a Rayleigh-Bénard Convection Cell, science vol. 298, 25 October

Krishnan M., Agrawal N., Burns M. A., Ugaz V. M. 2004. Reactions and Fluidics in Miniaturized Natural Convection Systems Anal. Chem. 76, 6254-6265

Mullis K. 1990. The unusual origin of the Polymerase Chain Reaction. Scientific American, pp. 56-65

Park N, Kim S, Hahn JH. 2003. Cylindrical compact thermal·cycling device for continuous-flow polymerase chain reaction. Anal Chem. 75: 6029-6033.

Wang W. , Li Z. X., Guo Z. Y. 2005. Numerical simulation of micro-flow-through PCR chip, Microscale thermophysical engineering, 9: 281-293.

Wheeler EK, Benett W, Stratton P, Richards J, Chen A et al. 2004. Convectively driven polymerase chain reaction thermal cycler. Anal Chem. 76, 4011-4016.